Article

Poly(ether ether ketone)-Induced Surface Modification of Polyethylene Separators for Li-Ion Batteries

Yunjung Kim [1], Yong-Jin Jang [1], Hyungeun Seo [1], Je-Nam Lee [2], Sang-Gil Woo [2,*] and Jae-Hun Kim [1,*]

[1] School of Materials Science and Engineering, Kookmin University, Seoul 02707, Republic of Korea
[2] Advanced Batteries Research Center, Korea Electronics Technology Institute, Seongnam 13509, Republic of Korea
* Correspondence: blackdragon@keti.re.kr (S.-G.W.); jaehunkim@kookmin.ac.kr (J.-H.K.)

Abstract: With the global effort to reduce fossil fuels and to use eco-friendly energy, interest in Li-ion batteries (LIBs) is rapidly increasing. In the LIB system, the separator is an important component for determining the rate performance and safety of cells. Although polyolefin separators are commercially used in LIBs, they still suffer from inferior electrolyte wettability and low thermal stability issues. Here, we introduce a chemical surface modification for polyethylene (PE) separators using a poly(ether ether ketone) (PEEK) coating. The separators were pretreated in a tannic acid solution to enforce the adhesion of the coated layers. Then, PEEK was coated onto the PE surface by a doctor blading method. The separators were examined by infrared spectroscopy, and the surface properties were characterized by electrolyte uptake and contact angle measurements. The treated surface was hydrophilic, and the ionic conductivity of the cell with the modified separator was significantly improved. As a result, the corresponding rate performance was significantly improved. The surface modification strategy proposed here can be applied to polyolefin-based separators as well.

Keywords: surface modification; Poly(ether ether ketone); hydrophilic; separator; Li-ion battery

1. Introduction

Li-ion batteries (LIBs) have been widely used in various applications such as electric vehicles and energy storage devices because of their advantages, which include a high energy density, long cycle life and moderate cost [1]. LIB cells consist of four major components: an anode, a cathode, an electrolyte, and a separator. The separator is placed between the cathode and the anode to prevent physical contact between the two electrodes and to enable ion transport through the electrolyte. To improve battery performance such as cycle performance, power density, and safety, upgrading the separator is considered an effective method. The physical and chemical properties of the LIB separator include high strength, good porosity, chemical resistance to electrolyte, wettability, and thermal durability. Among these properties, an excellent electrolyte wettability is essential to secure the electrochemical properties of cells [2–5]. Polyolefin-based separators such as polyethylene (PE) and polypropylene (PP) are commonly used in LIBs because of their excellent electrochemical stability and low costs; further, these separators can be mass produced by an optimized process. However, the wettability of these separators to electrolyte is not enough due to a low surface energy, which leads to poor electrolyte compatibility and rate performance. In addition, PE and PP separators have low melting points of 130 °C and 150 °C, respectively, which cannot protect the cells when thermal runaway occurs in LIBs [6,7].

Thus far, numerous methods have been reported to overcome the limitations of the PE separators. Surface modification methods with inorganic particle coating, such as Al_2O_3, SiO_2, and TiO_2 [8–10], and polymer coating, including the polyvinlylidene fluoride-hexafluoropropylene co-polymer, polyimide, and poly(methly methancylate) [11–13], have

been used to modify the separators. Although these coating methods can effectively improve the electrolyte compatibility, mechanical strength, and thermal stability of the separators, several shortcomings related to the coating process still remain unresolved. In particular, ceramic coating is a complex and costly process, and because of the weak adhesion between the inorganic coating particles and the separator, the particles detach from the separator when mechanical stress is generated during the cell assembly process. This may block the pores of the separator, interfere with the transfer of the Li ions, and degrade the cell performance. In the case of polymer coatings, extra processes such as heating and ultraviolet radiation are required to enhance the adhesion by an additional cross-linking procedure [14–16].

In this paper, we propose a facile poly(ether ether ketone) (PEEK) coating method to modify PE separators. PEEK is a kind of semi-crystalline polymer, which exhibits excellent intrinsic characteristics such as high chemical and thermal stability. In addition, the PEEK polymer may strongly interact with carbonate-based electrolytes, which are widely used in commercial LIBs, because of the existence of oxy-ether and polar carboxyl bonds in PEEK [17–19]. Tannic acid (TA) was introduced to improve the adhesion between the PE and PEEK layers. TA is an inexpensive polyphenol, which is synthesized from plants in abundant quantities and can self-polymerize in an alkalescence aqueous solution like dopamine. Further, it has five gallol groups and five catechol groups, and can thus form non-covalent bonds with various molecules through hydrogen or hydrophobic bonding. Based on these characteristics, TA was adopted as an intermediate layer or coating layer as reported in previous studies [20–23]. To modify the PE surface, the separator was pretreated with a TA solution using the dip-coating method, and a thin PEEK porous membrane was coated by a phase inversion process. After the surface modification, the wettability of the PE separator improved significantly, which in turn enhanced the electrochemical properties of the cell with the PE separator.

2. Experimental

Materials preparation: Before pretreatment in a TA solution, a commercial PE separator (16 μm, Tonen F16BME) was cleaned with ethyl alcohol in an ultrasonic bath for 30 min. Then, the cleaned separator was immersed into a tris-HCl buffer solution (pH 8.5) of TA (2 mg mL^{-1}, Sigma Aldrich, ACS reagent, Burlington, MA, USA) for 10 min. After the treatment, the separator was rinsed with deionized (DI) water several times and dried in a vacuum oven at 60 °C for 24 h. For the PEEK coating, poly(oxy-1,4-phenyleneoxy-1,4-phenylenecarbonly-1,4-phenylene) (PEEK, Sigma Aldrich, Burlington, MA, USA) was dissolved in a mixture solution of sulfuric acid and methyl sulfonic acid (weight ratio, 2:1) to prepare 12wt% casting solution. The solution was cast onto the pretreated PE separator using the doctor blade method. Subsequently, the PEEK-coated separator was immersed in DI water for 24 h. Finally, the prepared separator was dried in a vacuum oven at room temperature for 12 h.

Material characterization: The morphology of the separators was observed by field-emission scanning electron microscopy (FE-SEM, JEOL JSM-7401F, Japan). Fourier transform infrared (FT-IR, Bruker Vertex 70, Bruker, Germany) spectra of the separators were collected in the range of 1000–1800 cm^{-1}. The electrolyte contact angle was measured by a contact angle goniometer (CA, DSA30S, KRÜSS GmbH, Hamburg, Germany). The electrolyte uptake was calculated by measuring the weight of separator after dropping 1M LiPF$_6$ in an ethylene carbonate (EC)/diethyl carbonate (DEC) solution (3:7 by volume ratio, Panax Etec, Busan, Korea):

$$\text{Electrolyte uptake (\%)} = \frac{M_e - M_o}{M_o} \times 100 \tag{1}$$

M_o and M_e represents the weight of the separators before and after dropping the electrolyte, respectively. Thermal shrinkage was calculated by measuring the area of the separator after the heat treatment at each temperature for 30 min:

$$\text{Thermal shrinkage (\%)} = \frac{S_o - S}{S_o} \times 100 \tag{2}$$

S_o and S indicate the areas of the separator before and after heat treatment, respectively.

Electrochemical measurements: The electrochemical stability of the separator was evaluated by linear sweep voltammetry (LSV, BioLogic VSP, Grenoble, France) in the voltage range of 0–5 V at a scan rate of 1 mV s^{-1}. The cell was assembled by sandwiching a separator between stainless steel (SS) and a Li metal foil (SS/separator-electrolyte/Li). Electrochemical impedance spectroscopy (EIS) measurements were performed in the frequency range of 1 MHz to 100 mHz [24]. For the EIS measurements, a symmetric cell with a separator sandwiched between SS plates (SS/separator-electrolyte/SS) was assembled, and the ionic conductivity was calculated using the following equation:

$$\text{Ionic conductivity } (\sigma) = \frac{h}{R_b S} \tag{3}$$

where σ represents the ionic conductivity, R_b is the bulk resistance, h is the thickness of the separator, and S is the surface area of the separator. For the electrochemical cycle tests, coin-type cells (CR2032) were assembled in an argon-filled glovebox. The pristine or treated PE separator was sandwiched between a Li metal foil anode and a LiNi$_{0.8}$Co$_{0.1}$Mn$_{0.1}$O$_2$ (NCM811) cathode with 1M LiPF$_6$ in EC/DEC (3:7 by volume) as the electrolyte. For the cathode preparation, the active material (NCM811, 92wt%), a polyvinylidene fluoride binder (PVDF, 4wt%), and a conducting agent (i.e., carbon; Super P, 4wt%) were dissolved in an N-methyl-2-pyrrolidone solution. The slurry was coated onto an aluminum foil current collector. The electrode was roll-pressed and dried at 80 °C for 12 h. Galvanostatic charge and discharge cycling was performed within the potential window of 2.75–4.2 V (vs. Li$^+$/Li) at specific currents of 20–400 mA g^{-1} (1 C = 200 mA g^{-1}).

3. Results and Discussion

Figure 1 shows the schematic for surface modification of the PE separator. First, the pristine PE separator was pretreated in a TA solution. Then, the PEEK solution was cast onto the PE separator, and a thin PEEK layer was coated on the separator surface. In this process, self-polymerization possibly occurs between the TA and PEEK layers with aid of hydrogen bonds because of the TA pretreatment. The molecular structure of TA and sulfonated PEEK and the possible polymerization mechanism of the two substances are depicted in Figure 1. The pyrogallol or catechol group type phenols in TA can react with the sulfated PEEK [23], and based on this reaction, it can be expected that the PE surface was well coated with the PEEK layers. Figure 2 presents the FE-SEM images of the pristine and surface-treated PE separators. The samples pretreated in the TA solution and coated with PEEK are named as TA-PE and PEEK@TA-PE. After the TA treatment, the morphology of the PE separator did not show any significant changes. However, the surface of the PE fibrous structure was transformed into a smooth surface after the PEEK coating (Figure 2c). To confirm the coating, we performed the coating procedure five times. Then, the FE-SEM image was obtained (Figure 2d). From the image, the thicker PE fibers are observed, indicating that the PEEK coating was well conducted. The Gurley numbers of the pristine and PEEK@TA-PE separators were measured to be 214 and 223 s/100 mL, respectively, which supports that the porous structure of the PE separator was not significantly changed after the coating.
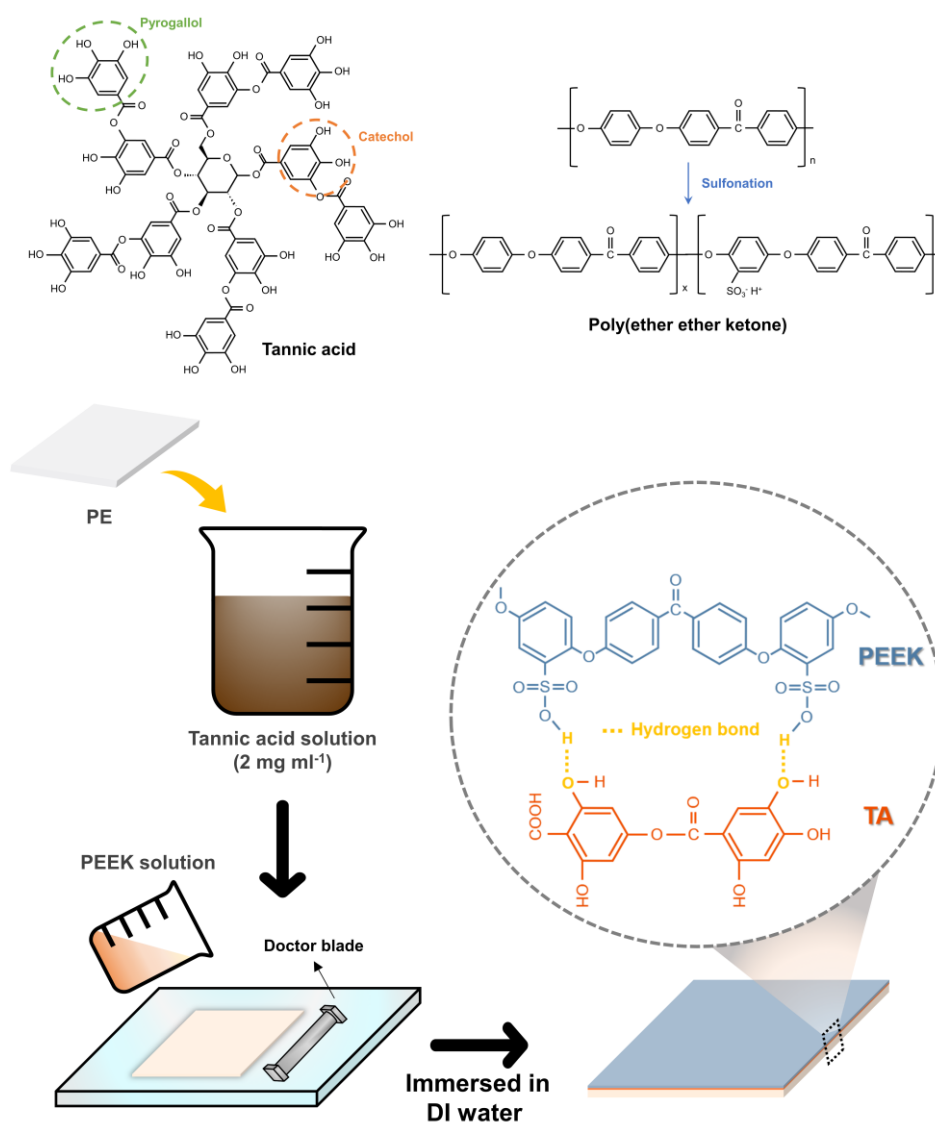
Figure 1. Chemical structures of TA and sulfonated PEEK; schematic of surface modification of the PE separator and possible reaction mechanism of TA and PEEK.
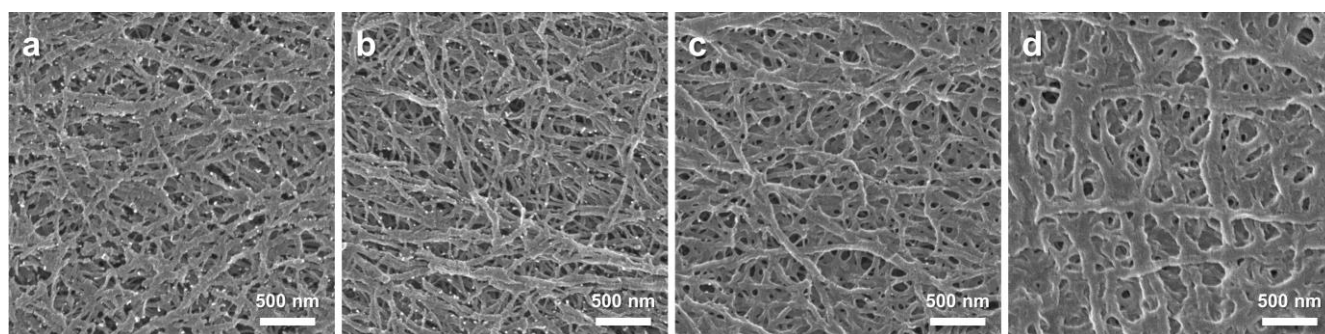

Figure 2. FE-SEM images of the (**a**) PE, (**b**) PE-TA, (**c**) PEEK@TA-PE, and (**d**) PE separators after the PEEK coating five times.

To confirm the effects of the TA pretreatment and PEEK layer, FT-IR spectra were collected, as shown in Figure 3, which shows few characteristic peaks corresponding to TA. The characteristic peak at approximately 1213 cm^{-1} could be attributed to the C–O stretching vibration of polyols [23,25], and those at 1607 and 1710 cm^{-1} correspond to

the C=C and C=O stretching vibrations in TA, respectively [23,26]. The spectrum of the PEEK-coated separator is distinct from that of the pristine PE separator. The characteristic peaks at 1031 and 1081 cm^{-1} can be ascribed to the S=O stretching and symmetric O=S=O bond in sulfonated PEEK, respectively [27–29]. The prominent peaks at 1224 and 1600 cm^{-1} correspond to the ether group stretching vibration and carbonyl stretching in PEEK, respectively [29,30]. From these FE-SEM and FT-IR analyses, it can be confirmed that the PEEK layer was well coated onto the PE separator.
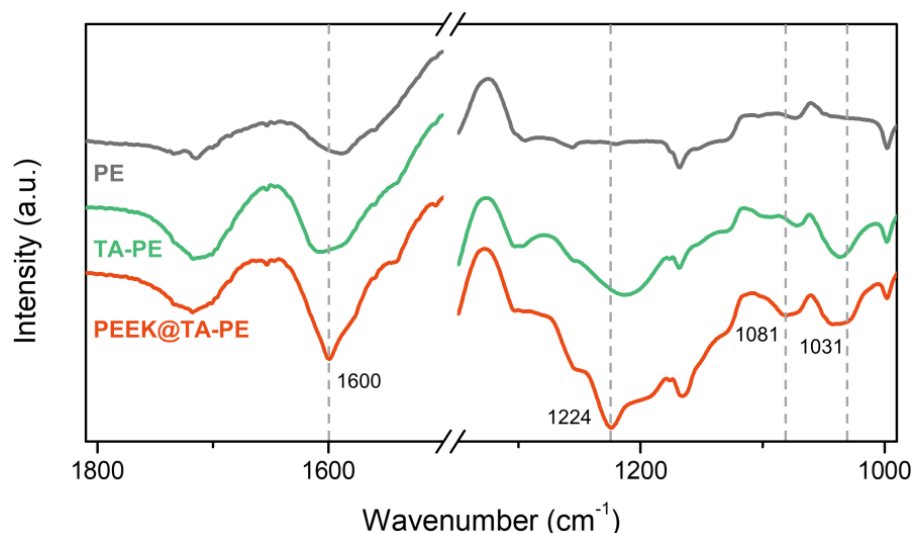

Figure 3. FT-IR spectra of the pristine PE, TA-PE, and PEEK@TA-PE separators.

Figure 4 shows digital photographs, which indicate the wettability of the separators. We dropped 1M LiPF$_6$ EC/DEC (electrolyte) on the pristine PE, TA-PE, and PEEK@TA-PE separators and measured the degree of wettability for 10 min. The corresponding results show that the PEEK-coated separator rapidly absorbed the electrolyte over the entire area after 1 min, whereas the pristine PE and TA pretreated separators exhibited much smaller wetted areas. These results indicate that the wettability of PE was enhanced by the PEEK coating because of the presence of several surface functional groups such as phenol group in TA and sulfur–oxygen and carbon–oxygen bonds in sulfonated PEEK. Upon surface modification, the surface of the PE separator became hydrophilic, and therefore, the improvement in the wettability can be attributed to the enhanced hydrophilic properties of the separators.
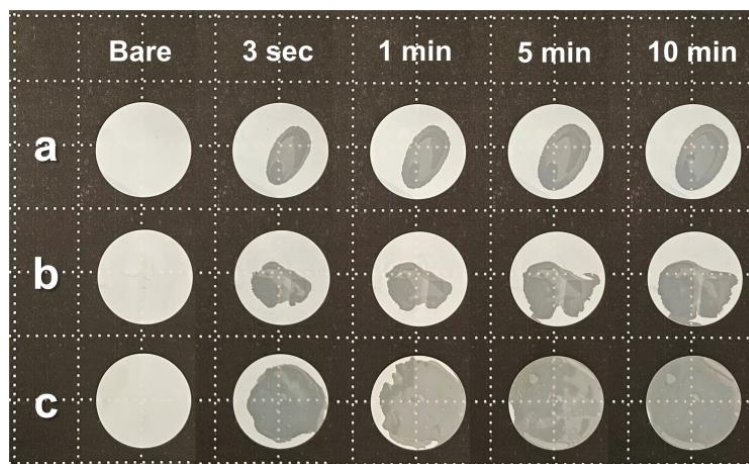

Figure 4. Digital photographs of the (**a**) PE, (**b**) TA-PE, and (**c**) PEEK@TA-PE separators after dropping the electrolyte.

Figure 5 presents the electrolyte uptake and contact angle measurement results. The calculated electrolyte uptake of the pristine PE, TA-PE, and PEEK@TA-PE samples are 46.1%, 62.1%, and 293%, respectively. The measured contact angle of the pristine PE sample is 28.4°, which decreases to 25.2° and 13.5° for the TA-PE, and PEEK@TA-PE samples, respectively, which support the previously mentioned calculated electrolyte uptakes of the samples. After the pretreatment in the TA solution and the PEEK coating, the surface became further hydrophilic; additionally, the electrolyte impregnation ability was greatly enhanced. These observations can be attributed to the physical properties of PEEK. The results of the aforementioned wettability tests confirmed that the surface of the PE separator transformed from hydrophobic to hydrophilic, and the electrolyte uptake was improved. Because of these two characteristics, the treated separators can be easily used in LIBs.
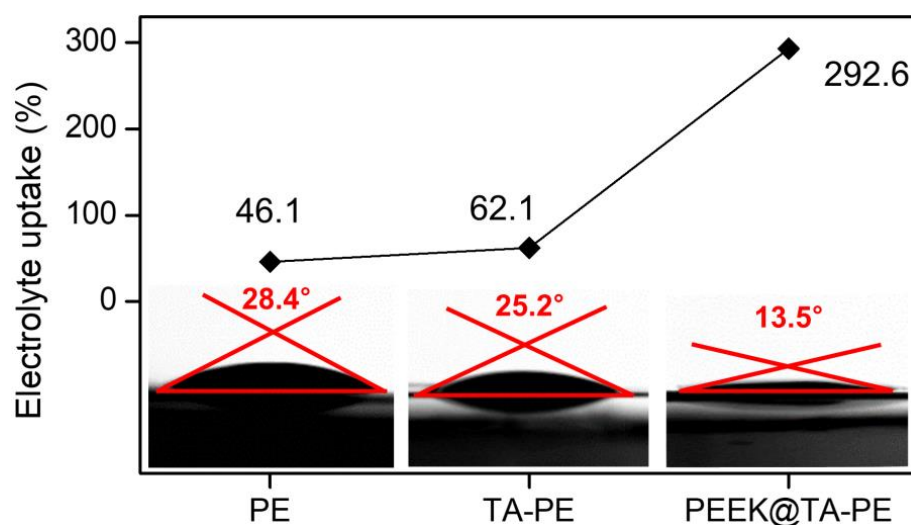

Figure 5. Electrolyte uptake and contact angle measurement results of the PE, TA-PE, and PEEK@TA-PE separators.

Further, we investigated the thermal properties of the PE separators. Figure 6a shows the digital photographs of the samples tested for thermal stability. A Thermal shrinkage test was performed to evaluate the thermal stability of the separators at high temperatures. The pristine PE, TA-PE, and PEEK@TA-PE samples were heated at 100 °C, 120 °C and 140 °C for 30 min, respectively. Even after heating at 100 °C and 120 °C, all the separators well maintained their shapes. However, a difference was observed at 140 °C; the PEEK@TA-PE sample retained its original shape after heating at this temperature, but the other two samples showed shape deformations. To examine the thermal properties, the area ratio to the samples that were not treated at high temperatures was calculated. Figure 6b shows the thermal shrinkage ratio obtained using Equation (2). The PE and TA-PE samples exhibit approximately 75% and 69% shrinkage, respectively. However, the PEEK-coated sample shows a shrinkage of only 43%. These results confirmed that the thermal stability of the PE separator can be improved by applying the PEEK coating process.

Figure 7 shows the EIS measurement results of the PE and PEEK@TA-PE separators. The Nyquist plots of the cell (SS/separator-electrolyte/SS) assembled with the PE and PEEK@TA-PE separators are shown in Figure 7a. The resistance values (x-axis intercept data) were used to calculate the ionic conductivity of the liquid electrolyte, and the corresponding results (obtained using Equation (3)) are shown in Figure 7b. The ionic conductivity values of the pristine PE and PEEK-coated separators are 4.3×10^{-4} and 6.3×10^{-4} S cm^{-1}, respectively, and this increase in the conductivity values can be attributed to the PEEK coating. The coating significantly changed the electrolyte wettability and also increased the ionic conductivity.
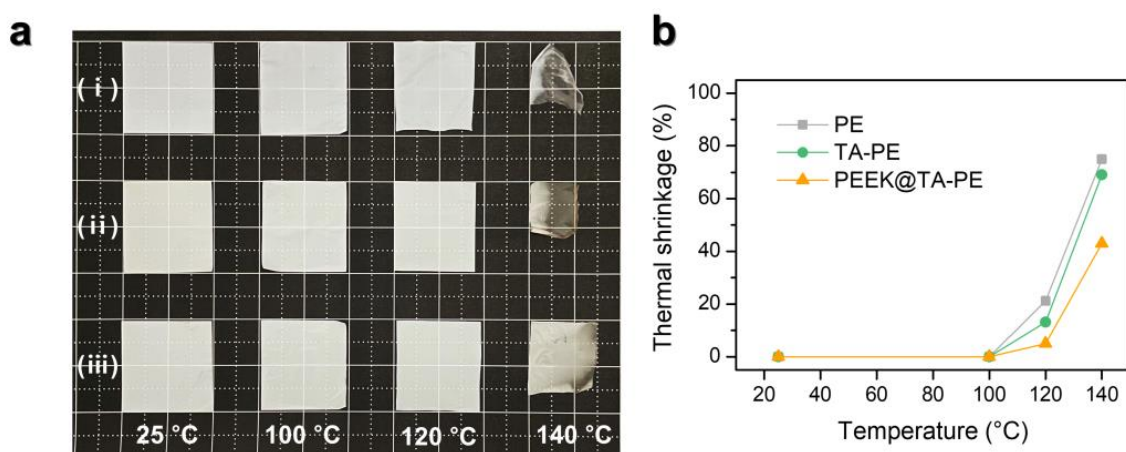
Figure 6. (**a**) Digital photographs of the (**i**) PE, (**ii**) TA-PE, and (**iii**) PEEK@TA-PE separators after heat treatment at each temperature; (**b**) thermal shrinkage calculation results.
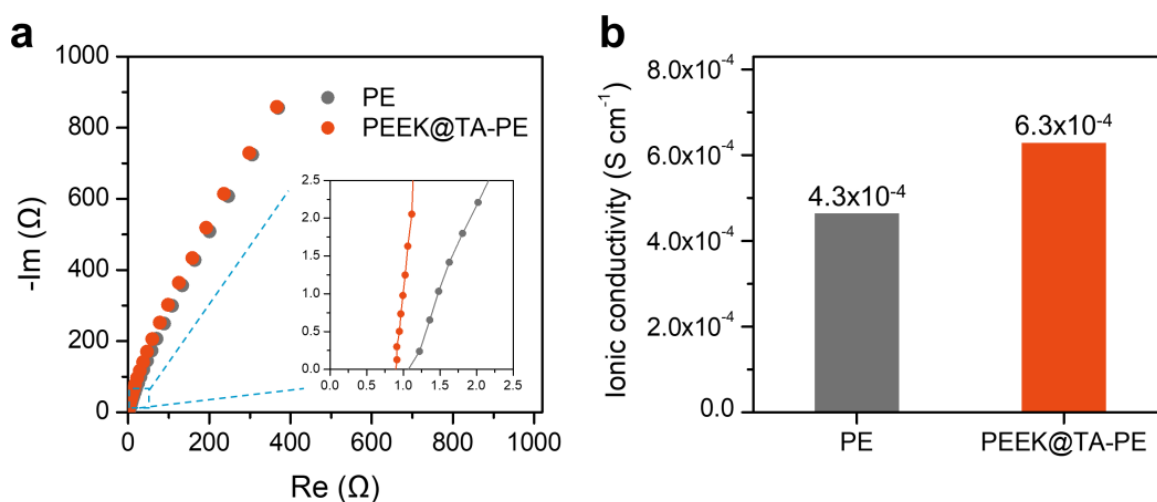

Figure 7. (**a**) Nyquist plots of the SS/separator-electrolyte/SS cells with the PE and PEEK@TA-PE separators; (**b**) calculated ionic conductivity results.

Figure 8 shows the electrochemical test results of the cells with the pristine and PEEK-coated separators. The LSV profiles of the cells with the PE and PEEK@TA-PE separators are shown in Figure 8a. Evidently, the profiles are flat for both the cells, implying that the cells with the separators are stable in the voltage range of 0–5 V. Figure 8b presents the galvanostatic discharge–charge curves of the cells with the PE and PEEK@TA-PE separators for the first two cycles. For both the cells, the initial charge and discharge capacities are approximately 200 and 170 mAh g^{-1}, respectively, and the initial Coulombic efficiency is 85%; the curves show the typical features of high-Ni layered cathodes. Figure 8c shows the cycling performance of the cells with the PE and PEEK@TA-PE separators, indicating even after 150 cycles, the capacities are well maintained for both the cells. Figure 8d presents the rate performance of the cells with the separators. At low rates of 0.1–0.2 C, the capacity difference is negligible. However, as the C-rate is increased to 0.5, 1.0, and 2.0 C, the reversible capacity changes. When the PEEK-treated separator was incorporated in the cell, the capacity was well maintained. The capacities of the cells with the PE and PEEK@TA-PE separators at a high rate of 2 C are 95 and 113 mAh g^{-1}, respectively. The improved rate performance can be assigned to the surface modification by the PEEK coating. After the coating, the surface becomes hydrophilic, and the ionic conductivity increases, which in turn significantly enhances the rate performance. Therefore, it can be concluded that the

surface modification of the PE separator is effective to enhance the rate performance of the cells.
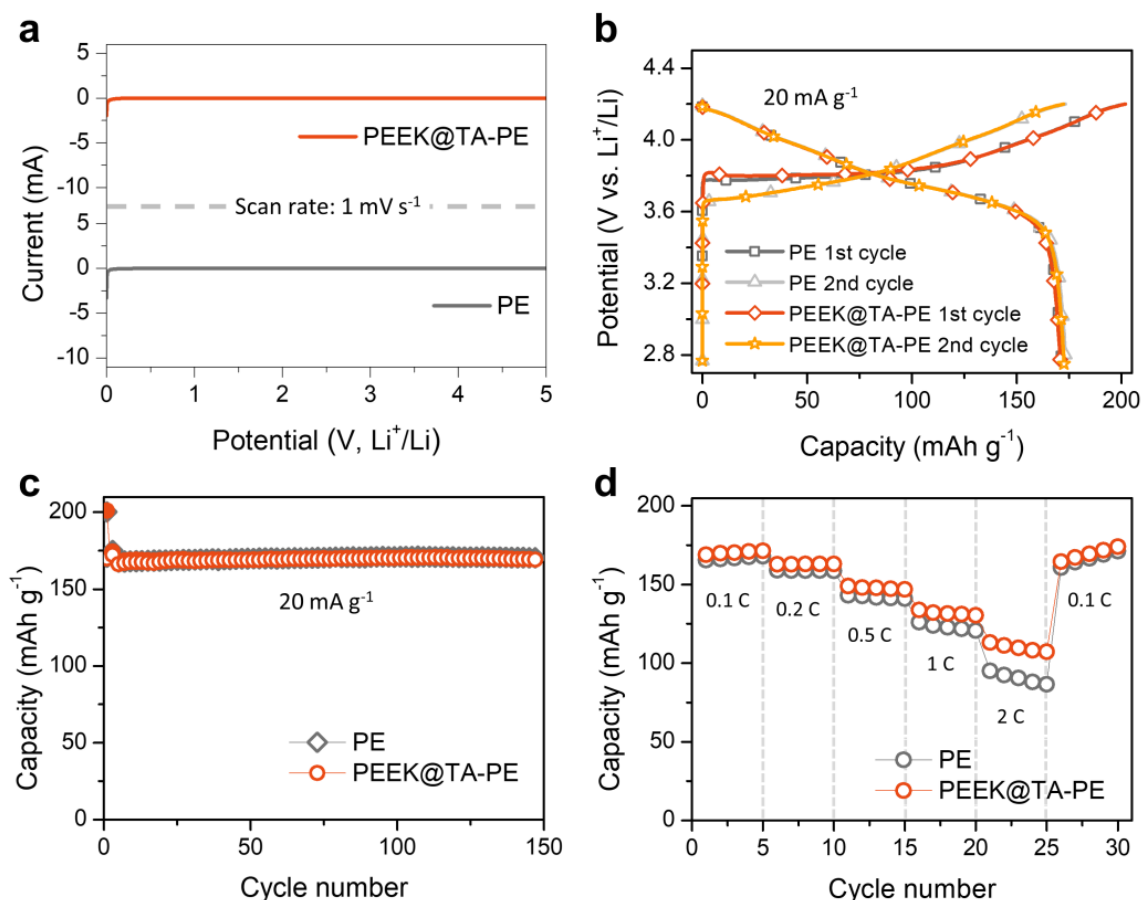

Figure 8. Electrochemical properties: (**a**) LSV curves, (**b**) voltage profiles at 20 mA g^{-1} (0.1 C), (**c**) cycle performance at 0.1 C, and (**d**) rate performance of the cells with the PE and PEEK@TA-PE separators.

4. Conclusions

We propose a facile method to modify the PE separators used in LIBs. In this case, the separator was first pretreated in a TA solution, and the sample was coated with PEEK; the PEEK coating was confirmed by FT-IR analysis. Because of the chemical modification by PEEK, the hydrophobic PE surface became hydrophilic, and the electrolyte wettability of the separator was significantly improved. The changes in surface property were examined through an electrolyte uptake test and contact angle measurements. The results showed that the ionic conductivity of the cell with the modified separator was significantly improved. The electrochemical test results demonstrated that the rate performance of the cell with the treated separator was greatly enhanced. These results can be attributed to the surface modification of the PE separator. Therefore, the proposed chemical treatment strategy can be applied to perform surface modification of polyolefin-based separators for LIBs.

Author Contributions: Conceptualization, Y.K. and J.-H.K.; methodology, Y.K.; validation, Y.K., Y.-J.J. and H.S.; investigation, Y.K., Y.-J.J., H.S. and J.-N.L.; data curation, Y.K, J.-N.L., S.-G.W. and J.-H.K.; writing—original draft preparation, Y.K.; writing—review and editing, J.-N.L., S.-G.W. and J.-H.K.; visualization, Y.K.; supervision, S.-G.W. and J.-H.K.; project administration, J.-N.L., S.-G.W. and J.-H.K.; funding acquisition, S.-G.W. and J.-H.K. All authors have read and agreed to the published version of the manuscript.

Data Availability Statement: Data available on request.

Conflicts of Interest: The authors declare no conflict of interest.

References

1. Nitta, N.; Wu, F.; Lee, J.T.; Yushin, G. Li-ion battery materials: Present and future. *Mater. Today* **2015**, *18*, 252–264. [CrossRef]
2. Arora, P.; Zhang, Z. Battery Separators. *Chem. Rev.* **2004**, *104*, 4419–4462. [CrossRef]
3. Zhang, S.S. A review on the separators of liquid electrolyte Li-ion batteries. *J. Power Sources* **2007**, *164*, 351–364. [CrossRef]
4. Huang, X. Separator technologies for lithium-ion batteries. *J. Solid State Electrochem.* **2011**, *15*, 649–662. [CrossRef]
5. Lee, H.; Yanilmaz, M.; Toprakci, O.; Fu, K.; Zhang, X. A review of recent developments in membrane separators for rechargeable lithium-ion batteries. *Energy Environ. Sci.* **2014**, *7*, 3857–3886. [CrossRef]
6. Heidari, A.A.; Mahdavi, H. Recent Development of Polyolefin-Based Microporous Separators for Li−Ion Batteries: A Review. *Chem. Rec.* **2020**, *20*, 570–595. [CrossRef]
7. Yoo, S.H.; Kim, C.K. Enhancement of the Meltdown Temperature of a Lithium Ion Battery Separator via a Nanocomposite Coating. *Ind. Eng. Chem. Res.* **2009**, *48*, 9936–9941. [CrossRef]
8. Shi, C.; Zhang, P.; Chen, L.; Yang, P.; Zhao, J. Effect of a thin ceramic-coating layer on thermal and electrochemical properties of polyethylene separator for lithium-ion batteries. *J. Power Sources* **2014**, *270*, 547–553. [CrossRef]
9. Shin, W.-K.; Kim, D.-W. High performance ceramic-coated separators prepared with lithium ion-containing SiO2 particles for lithium-ion batteries. *J. Power Sources* **2013**, *226*, 54–60. [CrossRef]
10. Juang, R.-S.; Hsieh, C.-T.; Chen, P.-A.; Chen, Y.-F. Microwave-assisted synthesis of titania coating onto polymeric separators for improved lithium-ion battery performance. *J. Power Sources* **2015**, *286*, 526–533. [CrossRef]
11. Kim, K.J.; Kim, J.-H.; Park, M.-S.; Kwon, H.K.; Kim, H.; Kim, Y.-J. Enhancement of electrochemical and thermal properties of polyethylene separators coated with polyvinylidene fluoride–hexafluoropropylene co-polymer for Li-ion batteries. *J. Power Sources* **2012**, *198*, 298–302. [CrossRef]
12. Wu, D.; Shi, C.; Huang, S.; Qiu, X.; Wang, H.; Zhan, Z.; Zhang, P.; Zhao, J.; Sun, D.; Lin, L. Electrospun Nanofibers for Sandwiched Polyimide/Poly (vinylidene fluoride)/Polyimide Separators with the Thermal Shutdown Function. *Electrochim. Acta* **2015**, *176*, 727–734. [CrossRef]
13. Park, J.-H.; Park, W.; Kim, J.H.; Ryoo, D.; Kim, H.S.; Jeong, Y.U.; Kim, D.-W.; Lee, S.-Y. Close-packed poly(methyl methacrylate) nanoparticle arrays-coated polyethylene separators for high-power lithium-ion polymer batteries. *J. Power Sources* **2011**, *196*, 7035–7038. [CrossRef]
14. Asghar, M.R.; Anwar, M.T.; Naveed, A. A Review on Inorganic Nanoparticles Modified Composite Membranes for Lithium-Ion Batteries: Recent Progress and Prospects. *Membranes* **2019**, *9*, 78. [CrossRef]
15. Song, J.; Ryou, M.-H.; Son, B.; Lee, J.-N.; Lee, D.J.; Lee, Y.M.; Choi, J.W.; Park, J.-K. Co-polyimide-coated polyethylene separators for enhanced thermal stability of lithium ion batteries. *Electrochim. Acta* **2012**, *85*, 524–530. [CrossRef]
16. Xing, J.; Li, J.; Fan, W.; Zhao, T.; Chen, X.; Li, H.; Cui, Y.; Wei, Z.; Zhao, Y. A review on nanofibrous separators towards enhanced mechanical properties for lithium-ion batteries. *Compos. B Eng.* **2022**, *243*, 110105. [CrossRef]
17. Liu, J.; Mo, Y.; Wang, S.; Ren, S.; Han, D.; Xiao, M.; Sun, L.; Meng, Y. Ultrastrong and Heat-Resistant Poly(ether ether ketone) Separator for Dendrite-Proof and Heat-Resistant Lithium-Ion Batteries. *ACS Appl. Energy Mater.* **2019**, *2*, 3886–3895. [CrossRef]
18. Li, D.; Shi, D.; Feng, K.; Li, X.; Zhang, H. Poly (ether ether ketone) (PEEK) porous membranes with super high thermal stability and high rate capability for lithium-ion batteries. *J. Membr. Sci.* **2017**, *530*, 125–131. [CrossRef]
19. Li, H.; Zhang, B.; Lin, B.; Yang, Y.; Zhao, Y.; Wang, L. Electrospun Poly(ether ether ketone) Nanofibrous Separator with Superior Performance for Lithium-Ion Batteries. *J. Electrochem. Soc.* **2018**, *165*, A939. [CrossRef]
20. Pan, L.; Wang, H.; Wu, C.; Liao, C.; Li, L. Tannic-Acid-Coated Polypropylene Membrane as a Separator for Lithium-Ion Batteries. *ACS Appl. Mater. Interfaces* **2015**, *7*, 16003–16010. [CrossRef]
21. Zhang, X.; Lv, Y.; Yang, H.-C.; Du, Y.; Xu, Z.-K. Polyphenol Coating as an Interlayer for Thin-Film Composite Membranes with Enhanced Nanofiltration Performance. *ACS Appl. Mater. Interfaces* **2016**, *8*, 32512–32519. [CrossRef]
22. Zhang, X.; Ren, P.-F.; Yang, H.-C.; Wan, L.-S.; Xu, Z.-K. Co-deposition of tannic acid and diethlyenetriamine for surface hydrophilization of hydrophobic polymer membranes. *Appl. Surf. Sci.* **2016**, *360*, 291–297. [CrossRef]
23. Zhang, Y.; Yuan, J.-J.; Song, Y.-Z.; Yin, X.; Sun, C.-C.; Zhu, L.-P.; Zhu, B.-K. Tannic acid/polyethyleneimine-decorated polypropylene separators for Li-Ion batteries and the role of the interfaces between separator and electrolyte. *Electrochim. Acta* **2018**, *275*, 25–31. [CrossRef]
24. Eftekharnia, M.; Hasanpoor, M.; Forsyth, M.; Kerr, R.; Howlett, C.-H. Toward Practical Li Metal Batteries: Importance of Separator Compatibility Using Ionic Liquid Electrolytes. *ACS Appl. Energy Mater.* **2019**, *2*, 6655–6663. [CrossRef]
25. Sheny, D.S.; Mathew, J.; Philip, D. Phytosynthesis of Au, Ag and Au–Ag bimetallic nanoparticles using aqueous extract and dried leaf of Anacardium occidentale. *Spectrochim. Acta A Mol. Biomol. Spectrosc.* **2011**, *79*, 254–262. [CrossRef] [PubMed]

26. Cumberland, S.L.; Strouse, G.F. Analysis of the Nature of Oxyanion Adsorption on Gold Nanomaterial Surfaces. *Langmuir* **2002**, *18*, 269–276. [CrossRef]
27. Ba, C.; Economy, J. Preparation and characterization of a neutrally charged antifouling nanofiltration membrane by coating a layer of sulfonated poly(ether ether ketone) on a positively charged nanofiltration membrane. *J. Membr. Sci.* **2010**, *362*, 192–201. [CrossRef]
28. Muthu Lakshmi, R.T.S.; Choudhary, V.; Varma, I.K. Sulphonated poly(ether ether ketone): Synthesis and characterisation. *J. Mater. Sci.* **2005**, *40*, 629–636. [CrossRef]
29. Fatarella, E.; Mylläri, V.; Ruzzante, M.; Pogni, R.; Baratto, M.C.; Skrifvars, M.; Syrjälä, S.; Järvelä, P. Sulfonated polyetheretherketone/polypropylene polymer blends for the production of photoactive materials. *J. Appl. Polym. Sci.* **2015**, *132*. [CrossRef]
30. Harris, L. A Study of the Crystallisation Kinetics in PEEK and PEEK Composites. Master's Thesis, University of Birmingham, Birmingham, UK, 2011.